Rios GS *et al*. (2024)
Notulae Botanicae Horti Agrobotanici Cluj-Napoca
Volume 52, Issue 1, Article number 13577
DOI:10.15835/nbha52113577
Research Article

Serra da Canastra National Park: Influence of forest fires on the RUSLE C factor and its impact on water erosion

Guilherme S. RIOS[1], Derielsen B. SANTANA[1], Guilherme H.E. LENSE[1], Felipe G. RUBIRA[2], Joaquim E.B. AYER[3], Ronaldo L. MINCATO[2*]

[1]*Federal University of Alfenas (UNIFAL-MG), Graduate Program in Environmental Sciences, R. Gabriel Monteiro da Silva, 700, Alfenas, Minas Gerais, Brazil; guilherme.rios@sou.unifal-mg.edu.br; derielsen.santana@sou.unifal-mg.edu.br; guilherme.lense@sou.unifal-mg.edu.br*
[2]*Federal University of Alfenas (UNIFAL-MG), Institute of Natural Sciences, R. Gabriel Monteiro da Silva, 700, Alfenas, Minas Gerais, Brazil; felipe.rubira@unifal-mg.edu.br; ronaldo.mincato@unifal-mg.edu.br (*corresponding author)*
[3]*University Center of Paulínia (UNIFACP), Department of Chemistry, R. Madre Maria Vilac, 121, Paulínia, São Paulo, Brazil; joaquimeba@gmail.com*

Abstract

The adverse impacts of soil degradation and nutrient loss resulting from water erosion are significant environmental concerns that have profound implications for both water quality and biodiversity. This study aims to evaluate the impact of forest fires on soil loss through water erosion in the Serra da Canastra National Park, in Minas Gerais state, Brazil. Using the Revised Universal Soil Loss Equation (RUSLE), which considers rainfall erosivity, soil erodibility, slope length and slope and vegetation cover, the C factor (vegetation cover) values were obtained from data from literature and methods based on the Normalized Differential Vegetation Index (NDVI). Validation was carried out using data on total sediment, water flow and daily runoff from the hydrosedimentological station and the InVEST software. The results highlight the significant impact of wildfires on soil loss through water erosion and indicate that areas recently affected by wildfires, especially on steep slopes and with more erodible soils, are subject to the highest rates of soil loss. Soil loss rates varied from 0.75 to 12.55 Mg ha^{-1} yr^{-1}, in part due to the different ways of obtaining factor C. The research emphasizes the need to conserve vegetation cover to prevent soil erosion, particularly in regions impacted by forest fires. This study offers valuable insights that can contribute to enhancing the sustainable environmental management of the Serra da Canastra National Park.

Keywords: Cerrado; conservation units; MapBiomas; remote sensing; vegetation index

Introduction

The Cerrado covers 24% of Brazilian territory, ranking as the country's second-largest biome, spanning 204 million ha (Sano *et al*., 2020). Despite being a global biodiversity conservation hotspot, it faces challenges from climate change and pressure from agricultural expansion, intensifying soil degradation, particularly

Received: 23 Dec 2023. Received in revised form: 24 Mar 2024. Accepted: 26 Mar 2024. Published online: 30 Mar 2024.
From Volume 49, Issue 1, 2021, Notulae Botanicae Horti Agrobotanici Cluj-Napoca journal uses article numbers in place of the traditional method of continuous pagination through the volume. The journal will continue to appear quarterly, as before, with four annual numbers.

through water erosion. One consequence is the loss of ecosystem services, even in protected areas like Conservation Units (UC) (Brasil, 2000; Klink and Machado, 2005; Silva *et al*., 2019).

Preserving the Cerrado safeguards ecosystems and contributes to environmental health. In this context, the Serra da Canastra National Park, established in 1972, is a full protection conservation unit (Unidade de Conservação de Proteção Integral) located in the Cerrado of Minas Gerais. The park is partially drained by the watersheds of the Paranaíba, the Rio Grande, and the São Francisco rivers (Brasil, 1972; 2000). The Serra da Canastra National Park faces environmental challenges arising from land use changes, including high rates of water erosion and recurrent forest fires. However, the park's challenging geographical conditions, such as high altitudes and slopes, hinder the prevention and combat of forest fires (Messias and Ferreira, 2017; 2019a).

Human activities accentuate soil degradation and contribute to water erosion (Bertol *et al.*, 2019). Erosion, in this context, is directly linked to forest fires that remove vegetation cover, intensifying raindrop impact, accelerating runoff, and reducing water infiltration (Messias and Ferreira, 2017; 2019a; Hysa *et al*., 2021; Rodrigues and Costa, 2021). Forest fires increase soil losses up, amplifying greenhouse gas emissions (Shakesby, 2011; Lal, 2020; Valkanou *et al*., 2022).

In this scenario, the intensification of land use changes leads to significant socioeconomic impacts, including a decrease in agricultural production (Dechen *et al*., 2015; Polidoro *et al*., 2021). Additionally, water erosion affects water bodies through sedimentation, pollution, and eutrophication (Bertol *et al.*, 2019). Modeling soil water erosion in Geographic Information Systems (GIS) allows estimating soil loss rates (Costea *et al*., 2022). The Revised Universal Soil Loss Equation (RUSLE), proposed by Renard *et al*. (1997), is widely employed for estimating soil loss rates in large areas and watersheds. The equation considers five factors: rainfall erosivity (R); soil erodibility (K); topography (LS); land cover and management (C) and conservation practices (P). Several studies have been conducted to assess the performance of water erosion prediction models in Brazilian soils (Batista *et al*., 2017; Nachtigall *et al*., 2020; Lense *et al*., 2021; Macêdo *et al.*, 2021; Santana *et al*., 2021). In RUSLE, the C factor reflects the influences of soil management, vegetation cover, and residual biomass on water erosion, playing an essential role in soil loss estimates (Renard *et al*., 1997; Bertol *et al.*, 2019; Lanorte *et al*., 2019).

Experimental plot studies link land use and land cover (LULC) changes to water erosion, highlighting anthropogenic influences and underscoring the importance of determining the C factor for soil loss rate estimates. However, such studies are often time-consuming and costly (Wischmeier and Smith, 1978; Bertol *et al.,* 2019). Due to these difficulties, C values can also be derived from literature data or through vegetation indices like the Normalized Difference Vegetation Index (NDVI) (Rouse *et al.*, 1974), Modified green-red vegetation index (MGRVI), and Visible Atmospherically Resistant Indices Green (ViGREEN) (Panagos *et al.*, 2015; Batista *et al*., 2017; Barbosa *et al*., 2019; Costa *et al*., 2020; Gil and Pacheco, 2020; Félix *et al*., 2023). In this scenario, the objectives of this work were to quantify forest fires in the Serra da Canastra National Park from 2019 to 2021 and evaluate their impact on the RUSLE C factor and soil loss due to water erosion.

Materials and Methods

Study area

The Serra da Canastra National Park is situated in the south-southwest region of Minas Gerais State, covering 197,787 ha (Brasil, 1972), with 93,000 ha designated as a full protection conservation unit (Brasil, 2000). The full protected area aims to preserve endemic species of flora and fauna and environmental and ecosystem services through the imposition of strict rules, while unregulated areas face challenges arising from unsustainable agricultural management practices, such as recurrent forest fires (Brasil, 2005) (Figure 1).

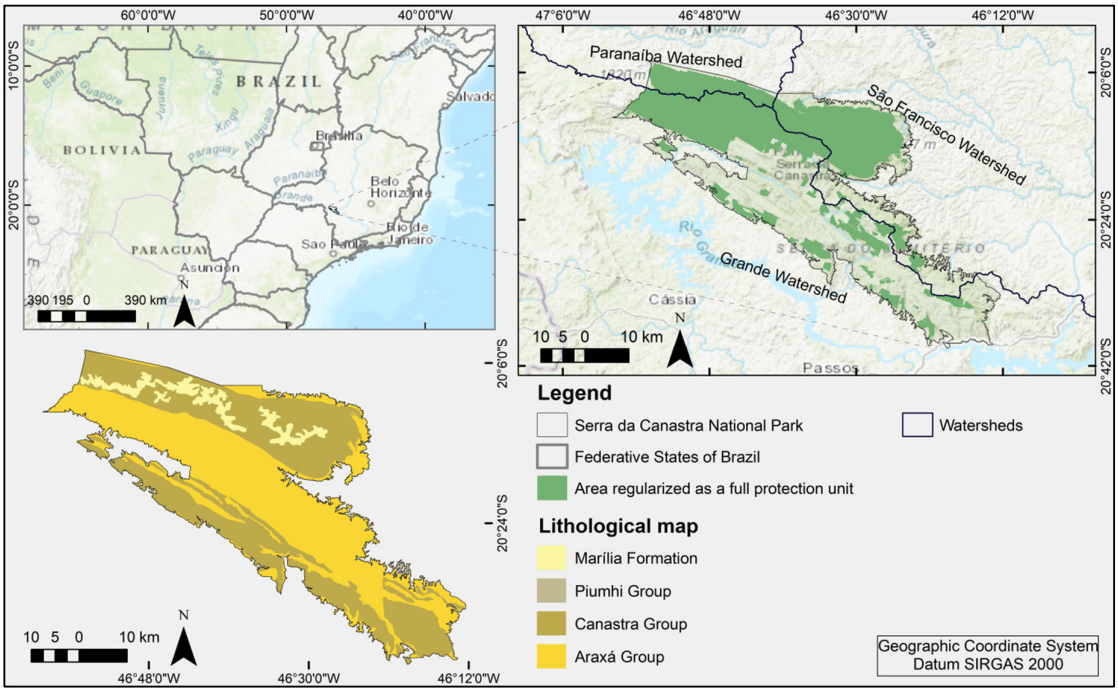

Figure 1. Location map of the Serra da Canastra National Park

The park preserves essential ecosystem services for the well-being of populations and protects endemic flora and fauna species. Covers partially the watersheds of Paranaíba, Rio Grande and São Francisco rivers (Brasil, 2005; Cardoso *et al.*, 2019).

The Serra da Canastra National Park features complex geology, characterized by Archean remnants of the Piumhi Group, succeeded by Mesoproterozoic metasedimentary rocks of the Canastra Group and Neoproterozoic rocks of the Araxá Group. These formations are partially covered by Phanerozoic sedimentary rocks of the Marília Formation from the Paraná Basin (Hasui, 2010; Salgado *et al.*, 2019; Silva *et al.*, 2020).

The park's topography ranges from 700 to 1,400 m, with morphostructural compartments marked by alternating plateaus and the presence of thrust and strike-slip faults (Messias and Ferreira, 2019b; Salgado *et al.*, 2019).

The predominant soils, according to the UFV *et al.* (2010) and the World Reference Base for Soil Resources (WRB) correlates (IUSS, 2015), are Dystrophic Litholic Neosols (Leptosols) and Dystrophic Argiluvic Plinthosols (Plinthosols), which cover 65% of the park. Additionally, there are Haplic Cambisol (Cambisols), Dystrophic Red Oxisol (Ferralsols), Dystrophic Red-Yellow Latosol (Ferralsols) and Eutrophic Red-Yellow Argisol (Acrisols) in a smaller proportion.

The region's climate, according to Köppen, is Cwa (humid subtropical climate) and Cwb (subtropical highland climate) types, characterized by hot summers and mild winters (Alvares *et al.*, 2013). Rainfall ranges between 1,000 and 1,800 mm, with temperatures fluctuating between 18 and 22 °C (Novaes *et al.*, 2018).

The Serra da Canastra generally features a phytophysionomy composed of low, twisted trees with irregular and contorted branches, with shrubs and sub-shrubs. It consists of species with perennial roots, enabling regrowth after burns (Brasil, 2005; Coutinho, 2006).

Methodology

The study comprised four stages: (1) acquisition of the cartographic base; (2) data processing, soil loss modeling, and result validation; (3) data treatment in spreadsheet environment; and (4) obtaining soil loss rates, as illustrated at Figure 2.

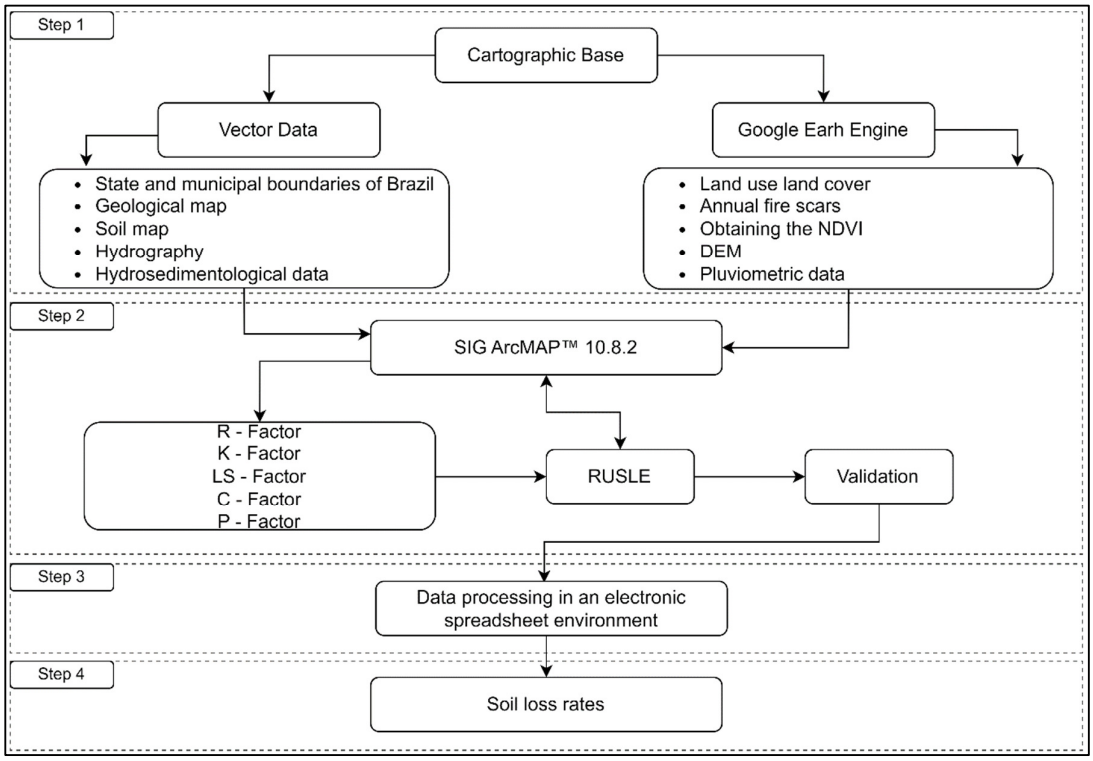

Figure 2. Flowchart of the research methodological process

In step 1, was obtained: the cartographic base (IBGE, 2022); the geological map of the area (Hasui, 2010); the soil map of Minas Gerais (UFV *et al*., 2010); hydrography data (ANA, 2023) and the Shuttle Radar Topography Mission (SRTM) Digital Elevation Model (DEM) with 30 m spatial resolution (Farr *et al*., 2007). The files were processed using ArcMap™ 10.8.2 (ESRI, 2021).

Wildfire scars and rainfall data from 2019 to 2021 were incorporated into the analysis. Fire data and LULC data for the Serra da Canastra National Park were obtained from the MapBiomas Fire Project – Collection 2 database (Mapbiomas, 2022) and the Annual Series Collection 7 of Land Use and Cover Maps of Brazil (Mapbiomas, 2023). The files were processed in a cloud computing environment using the toolkit on the Google Earth Engine platform (Gorelick *et al*., 2017). Precipitation data were acquired from the Climate Hazards Group InfraRed Precipitation - CHIRPS 2.0 satellite (Funk *et al*., 2015), due to the absence of a registered hydrometeorological station in the area (ANA, 2023).

In step 2, soil losses were modeled and validated. Water erosion soil losses were assessed using the Revised Universal Soil Loss Equation (RUSLE) (Renard *et al*., 1997) (Equation 1).

$$A = R \times K \times LS \times C \times P \quad \text{(Equation 1)}$$

Where: A is the average annual soil loss estimate (Mg ha^{-1} yr^{-1}); R is the rainfall and runoff erosivity factor (MJ mm ha^{-1} h^{-1} yr^{-1}); K is the soil erodibility factor (Mg ha^{-1} MJ^{-1} mm^{-1}); LS (length and slope) is the topographic factor (dimensionless); C is the soil cover management factor (dimensionless); and P is the soil conservation practice factor (dimensionless).

The ability of rain to cause erosion, due to the impact of raindrops on the soil and runoff, is determined by the R factor. The R factor was obtained from the rain erosivity map of the Minas Gerais State (Souza et al., 2022).

The K factor reflects the susceptibility of soils to erosion processes and was obtained from Batista *et al*. (2017), Cabral *et al*. (2005), Farinasso *et al*. (2006), Mannigel *et al*. (2002), Morais and Sales (2017) and Silva *et al*. (2009). The K values were inserted into the attribute table of the soil map shapefile, which was converted to a raster with a spatial resolution of 30 m by ArcMap™ 10.8.2 (ESRI, 2021).

The LS factor was modeled by Moore and Burch (1986) to determine the LS factor in complex terrains (Equation 2). The LS factor was processed from a DEM with a spatial resolution of 30 m using the raster calculator module in ArcMap™ 10.8.2 (ESRI, 2021).

$$LS = \frac{(FA \times ResDEM)}{22.13^{0.4}} \times \left(\frac{\sin S}{0{,}0896}\right)^{1.3} \quad \text{(Equation 2)}$$

Where: LS is the topographic factor; FA is the flow accumulation expressed as the number of grid cells in the DEM; S is the slope of the area in degrees, and ResDEM is the spatial resolution of the DEM (m).

The C factor varies from 0 to 1 and is a measure of the effectiveness of vegetation cover in protecting the soil against water erosion. Values close to 1 indicate low or no vegetation cover and those close to 0 reflect greater soil protection by the canopy.

The NDVI formula, derived from the ratio to determine the C factor, was employed using three approaches. In the first, values determined in experimental plots and available in the literature were utilized (C-Lit). In the other approaches, the NDVI spectral index was used, following the models proposed by Durigon *et al*. (2014) (Cr factor) and Macedo *et al*. (2021) (Cr2 factor).

The surface reflectance values of the red (R) and near-infrared (NIR) bands, as proposed by Rouse *et al*. (1974) (Equation 3):

$$NDVI = \frac{NIR - R}{NIR + R} \quad \text{(Equation 3)}$$

Where: NDVI is the Normalized Difference Vegetation Index (dimensionless); NIR is the Near-Infrared surface reflectance (dimensionless); R is the red surface reflectance (dimensionless).

The Durigon *et al*. (2014) method is described by Equation 4.

$$Cr = \frac{(-NDVI + 1)}{2} \quad \text{(Equation 4)}$$

Macedo *et al*. (2021) method is an adaptation of Equation 4 and considers seasonality and precipitation. For this, the variables Pptx (accumulated precipitation in the quarter before the first scene to calculate NDVI) and Lv (average accumulated precipitation in the quarter following the first scene) are used. Thus, when Lv is lower or equal to Pptx, there is less presence of low-reflectance dry vegetation. In this case, it is necessary to obtain the Cr2 factor (Equation 5).

$$Cr2 = \frac{(-NDVI + z)}{2z} \quad \text{(Equation 5)}$$

Where: z represents the pixel with the maximum NDVI value.

Thus, when Lv is greater than Pptx, drier vegetation is expected due to seasonality. In this case, the CPC factor (Equation 6) is used to increase NDVI values based on precipitation, which allows the reclassification of dry vegetation targets considered as exposed soil.

$$CPC = Cr2\left(\frac{Pptx}{Lv}\right)^{H} \quad \text{(Equation 6)}$$

Where: H is the percentage of the pixel area in a situation of low NDVI due to seasonality (Equation 7).

$$H = \frac{(NDVIPC - NDVI)}{100} \quad \text{(Equation 7)}$$

Where: NDVIPC is the precipitation correction obtained by Equation 8.

$$NDVIPC = NDVI\frac{Lv}{PPtx} \quad \text{(Equation 8)}$$

The Cr2 calculations involved the processing of precipitation data obtained from the CHIRPS 2.0 satellite (Funk *et al*., 2015).

To obtain the NDVI C factor were used images from Landsat 8 from the OLI sensor, scenes 219/74 and 220/74, Collection 2 and Level 2, with a spatial resolution of 30 m (USGS, 2019). This data includes geometric and atmospheric corrections using the LaSRC 3.0 method (Zanter, 2019). Quarterly average NDVI values were derived from image processing in Google Earth Engine. Adjustments were also made to the scale factor, cloud mask and cloud shadow using the Fmask algorithm, which excluded cloud reflectance values (Zhu and Woodcock, 2014).

To capture seasonality, 102 scenes were processed, around 34 per year, providing broad intra-annual spectral coverage. This seasonal variation is consistent with the positive correlation between NDVI and soil water availability (Pettorelli *et al*., 2005; Nanzad *et al*., 2019). Thus, the images result from quarterly averages, which allow the identification of phenological changes, including those affected by forest fires.

The P factor varies from 0 to 1 and indicates the potential of conservation practices in reducing water erosion, with values close to 0 indicating efficient conservation practices (Beskow *et al*., 2009). P values were determined from the literature, through experimental plots, with values of 0.20 for forest formation, 0.50 for coffee and citrus, 0.56 for Cerrado formation, grassland, forestry, pasture, soybean, sugarcane, mosaic of uses and other temporary crops, and 1 for bare soil (Bertol *et al*., 2001; Martins *et al*., 2010; Andrade *et al*., 2011; Bertoni and Lombardi Neto, 2012; Senanayake *et al*., 2022).

The results were validated according to Beskow *et al.* (2009) and Batista *et al*. (2017), with data on transported sediments, water flow and daily runoff from hydrosedimentological station number 40037000 (ANA, 2023).

The modeling of soil losses by RUSLE does not differentiate between the fraction deposited on the terrain and that reaching water bodies. To overcome this, we integrated the model with the sediment delivery ratio (SDR) to water bodies. For this purpose, we utilized InVEST 3.14 software (Sharp *et al*., 2018), following the approach outlined by Vigiak *et al*. (2012).

Results and Discussion

The land use and land cover changes in the Serra da Canastra National Park from 2019 to 2021 are illustrated in Figure 3.

The quantification of land use and land cover data from 2019 to 2021 is presented in Table 1.

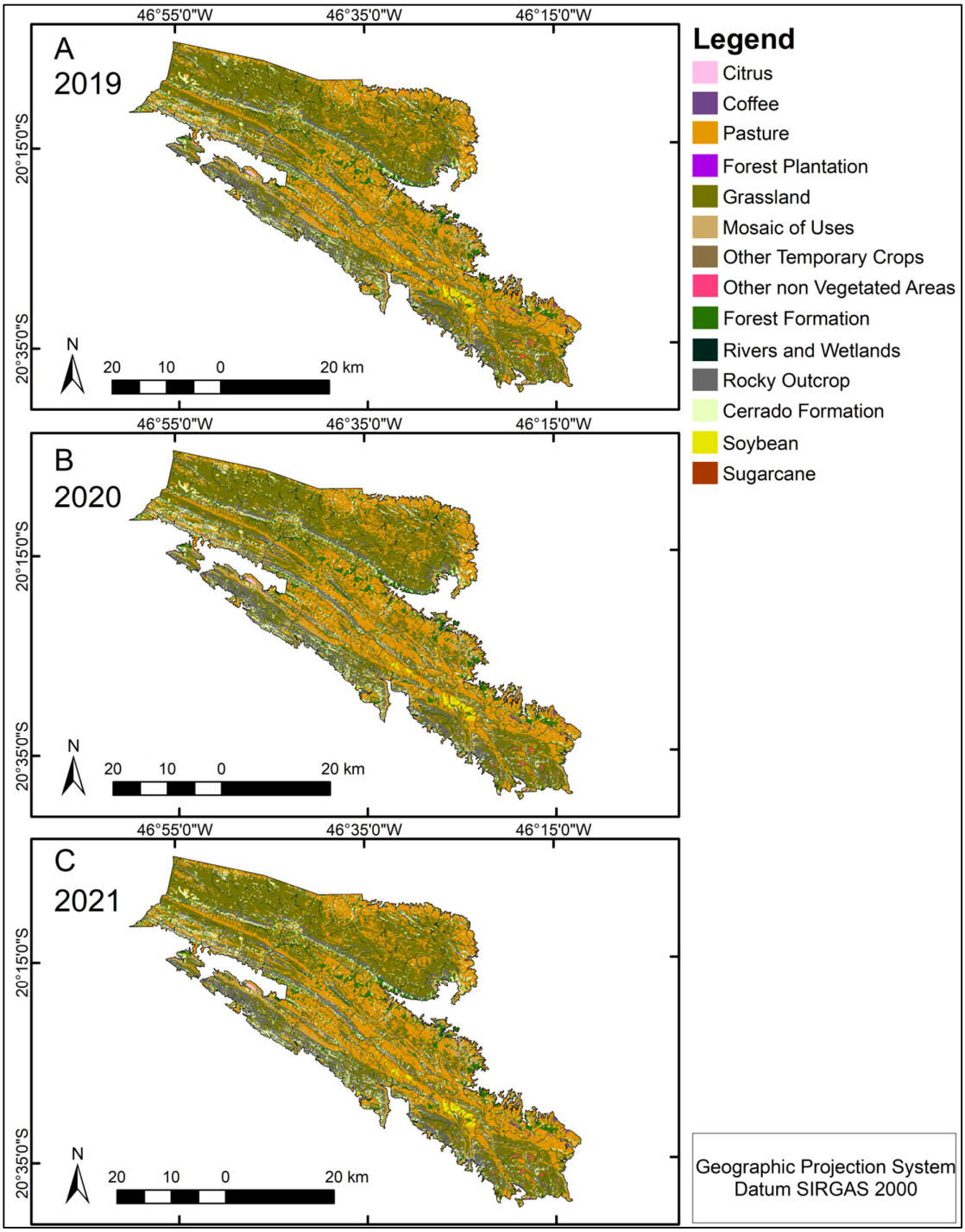

Figure 3. Land use and land cover map of the Serra da Canastra National Park. (A) 2019; (B) 2020; (C) 2021

Table 1. Area of land use and land cover classes in hectares (ha) and their respective percentages (%) (Mapbiomas, 2023)

Classes	2019		2020		2021	
	ha	%	ha	%	ha	%
Forest plantation	-	0.00	0.51	0.00	0.90	0.00
Sugarcane	6.72	0.01	6.72	0.00	5.64	0.00
Citrus	115.45	0.06	115.18	0.06	119.11	0.06
Other temporary crops	196.91	0.10	155.87	0.08	143.68	0.07
Other non-vegetated areas	277.95	0.14	272.41	0.14	278.89	0.14
Coffee	428.35	0.22	438.90	0.22	440.25	0.22
Soybean	1013.09	0.51	1144.97	0.58	1159.24	0.59
Mosaic of uses	5500.54	2.78	5513.54	2.79	5665.45	2.86
Rivers and wetlands	7121.88	3.60	7169.04	3.62	7021.99	3.55
Forest formation	12561.11	6.35	12626.66	6.38	12515.39	6.33
Cerrado formation	17298.03	8.75	17313.03	8.75	17178.05	8.69
Rocky outcrop	19974.27	10.10	19979.61	10.10	19991.18	10.11
Pasture	61565.73	31.13	61223.29	30.95	62497.35	31.60
Grassland	71712.60	36.26	71840.65	36.32	70741.13	35.77

Historically, forest fires have been recurrent in the Cerrado, particularly in the Serra da Canastra National Park, representing a serious threat to the preservation of its environmental and ecosystem services (Durigan and Ratter, 2015; Messias and Ferreira, 2019b). In the park, the unregulated areas are those most affected by the fires. Furthermore, they concentrate places with a high recurrence of forest fires, especially at higher altitudes, where there is a predominance of rural physiognomies, which facilitate the spread of fire in the dry season (Messias and Ferreira, 2019b). In the historical series considered, in 2019, fire scars covered 28,166 ha or 14% of the area, in 2020, 61,793 ha or 31%, and in 2021, 7,502 ha or 4% of the park area (Figure 4).

In the park, in 2019, the land use and occupation classes that presented the largest burned areas were: grassland formation with 11,278 ha or 5.7%, pasture with 9,422 ha or 4.8%, and Cerrado formation with 2,268 ha or 1.1% (Figure 4A). In 2020, there was the largest burned area in the park, with grassland formation covering 27,684 ha or 14%, pastures with 12,212 ha or 6.2%, and Cerrado formation with 7,245 ha or 3.7% (Figure 4B). Nevertheless, scars decreased significantly in 2021 and the classes with the largest forest fire areas were grassland formation with 3,264 ha or 1.7%, pastures with 1,530 ha or 0.8%, and Cerrado formation with 983 ha or 0.5% (Figure 4C).

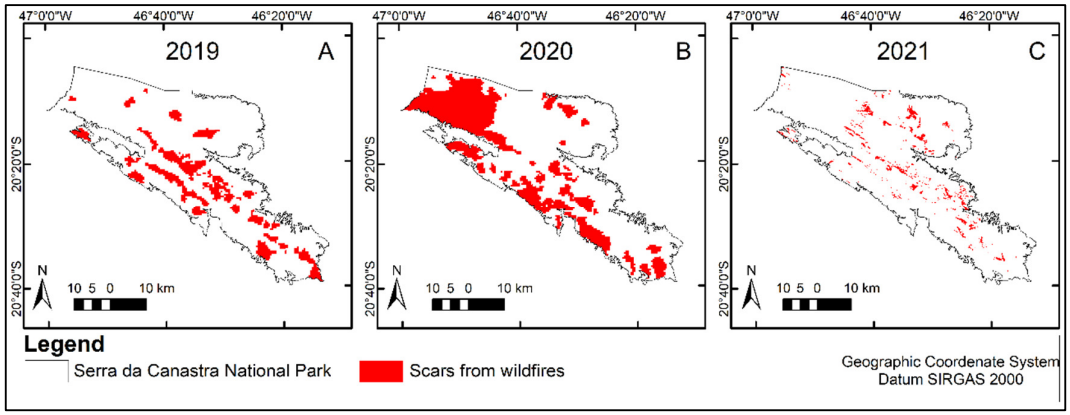

Figure 4. Scars from wildfires in the Serra da Canastra National Park. (A) 2019; (B) 2020; (C) 2021

The R factor ranged from 7132.06 to 8401.50 MJ mm ha^{-1} year $^{-1}$, with lower values predominating in the south/southeast of the park. Erosivity ranged from moderate to strong (Mello *et al.*, 2013) (Figure 5A).

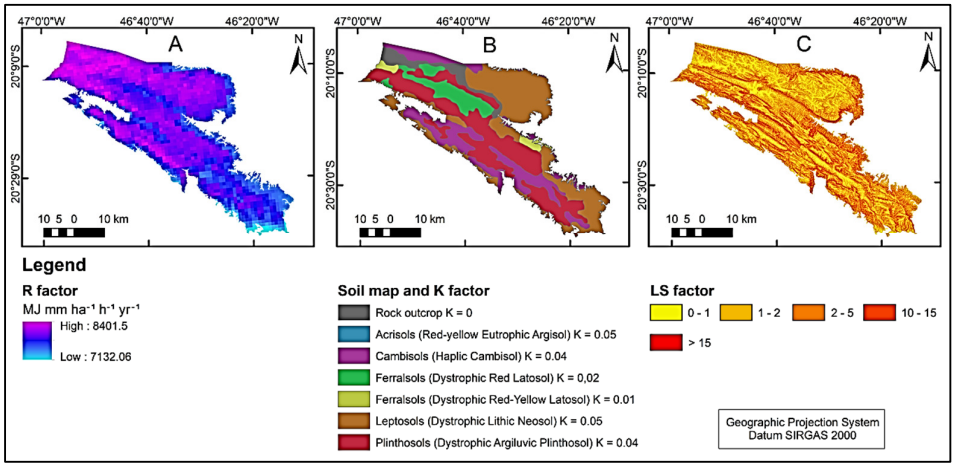

Figure 5. RUSLE factors in the study area. (A) R factor; (B) K factor; (C) LS factor

The park shows high erodibility (Figure 5B). The highest values are observed in Leptosols (Dystrophic Lithic Neosol), covering 34% of the area (Figure 5B). Plinthosols (Dystrophic Argiluvic Plinthosol) and Cambisols (Haplic Cambisol) cover 31% and 18% of the park, respectively, with K value of 0.04 Mg ha^{-1} MJ^{-1} mm^{-1}.

The distribution of LS intervals reveals that 64% of the area has values below 5 and 16% above 10 (Figure 5C), indicating moderate and high vulnerability to water erosion, respectively (Beskow *et al.*, 2009) (Table 2).

Table 2. Intervals of the LS factor for the Serra da Canastra National ParkInterval

Interval	Area (ha)	%
0-1	73,049.79	37
1-2	14,519.64	7
2-5	40,217.70	20
5-10	37,852.42	19
10-15	15,760.53	9
>15	16,242.32	8

The C-Lit factor was obtained from experimental plots in different areas described in the literature (Table 3).

Table 3. Soil cover management factor values (C-Lit factor)

Classes	C-Lit Factor	Reference
Forest formation	0.0004	Silva *et al.* (2010)
Cerrado formation	0.0020	Cunha *et al.* (2017)
Forest plantation	0.0470	Martins *et al.* (2010)
Grassland	0.0380	Cunha *et al.* (2017)
Pasture	0.1000	Roose (1977)
Sugarcane	0.1420	Andrade *et al.* (2011)
Mosaic of uses	0.1400	Ayer *et al.* (2015)
Other non-vegetated areas	1.0000	Roose (1977)
Soybean	0.1437	Bertol *et al.* (2001)
Other temporary crops	0.1500	Ayer *et al.* (2015)
Coffee	0.1350	Silva *et al.* (2010)
Citrus	0.1350	Silva *et al.* (2010)

Despite presenting lower values for the C factor, C-Lit considers a single value for each land-use class with homogeneous vegetative cover. The C factors derived from NDVI better represent phenological and seasonal variations in coverage, such as droughts and forest fires, as they identify changes in vegetative density within the same land-use class (Almagro *et al*., 2019) (Table 4).

Table 4. C factor values obtained from NDVI. Source: Cr factor from Durigon *et al*. (2014) and Cr2 from Macedo *et al*. (2021)

Classes	2019		2020		2021	
	Cr	Cr2	Cr	Cr2	Cr	Cr2
Forest formation	0.11	0.07	0.13	0.08	0.13	0.08
Cerrado formation	0.21	0.18	0.26	0.24	0.22	0.18
Forest plantation	-	-	0.10	0.05	0.12	0.06
Grassland	0.27	0.24	0.31	0.30	0.28	0.25
Pasture	0.25	0.21	0.28	0.26	0.26	0.22
Sugarcane	0.28	0.26	0.32	0.30	0.31	0.27
Mosaic of uses	0.21	0.18	0.25	0.23	0.23	0.19
Other non-vegetated areas	0.36	0.34	0.36	0.35	0.36	0.33
Soybean	0.27	0.21	0.22	0.19	0.29	0.27
Other temporary crops	0.25	0.21	0.30	0.28	0.28	0.24
Coffee	0.19	0.13	0.12	0.17	0.17	0.13
Citrus	0.29	0.23	0.20	0.23	0.27	0.24
Average	0.22	0.20	0.22	0.23	0.21	0.21

The average values of the Cr and Cr2 factors were slightly higher in 2020, suggesting that forest fires were the cause of the NDVI increase values. The largest fire scars show warmer colors on the maps (Figures 6E and 6H). For C-Lit, the majority occurs in lower value ranges, which results in the homogenization of land use and land cover classes in the cartographic representation (Figures 6A, 6B and 6C).

The highest average soil loss rate, 71.84 Mg ha^{-1} year $^{-1}$, was obtained in non-vegetated areas based on the C-Lit factor (Table 5). In 2020, soil losses followed the same pattern as in 2019. With C-Lit, the lowest soil losses were in the Forest plantation, with 0.11 Mg ha^{-1} yr^{-1}. Using the Cr and Cr2 factors, the average soil loss rates in 2020 were the highest. Compared to 2019, they were higher by 0.05% with the Cr factor and 0.26% with the Cr2 factor. Compared to 2021, they were higher by 0.05% for Cr and 0.15% for Cr2.

The highest soil loss rates in the time series were observed in cultivated areas, pastures, and non-vegetated areas, which are more vulnerable to erosive processes due to lower vegetation density compared to forests. In 2021, the estimated soil loss rates were the lowest for the different C factors used, reflecting the reduction in forest fires and the consequent increase in soil protection by vegetation cover (Gwapedza *et al*., 2021; Castro *et al*., 2022).

Areas with more fragile soils, rugged terrain, low canopy or no vegetation cover, and without conservation practices exhibited higher rates of soil loss (Liu *et al*., 2020; Lense *et al*., 2021; Santana *et al*., 2021). The spatial distribution of areas most susceptible to water erosion is illustrated in Figure 7.

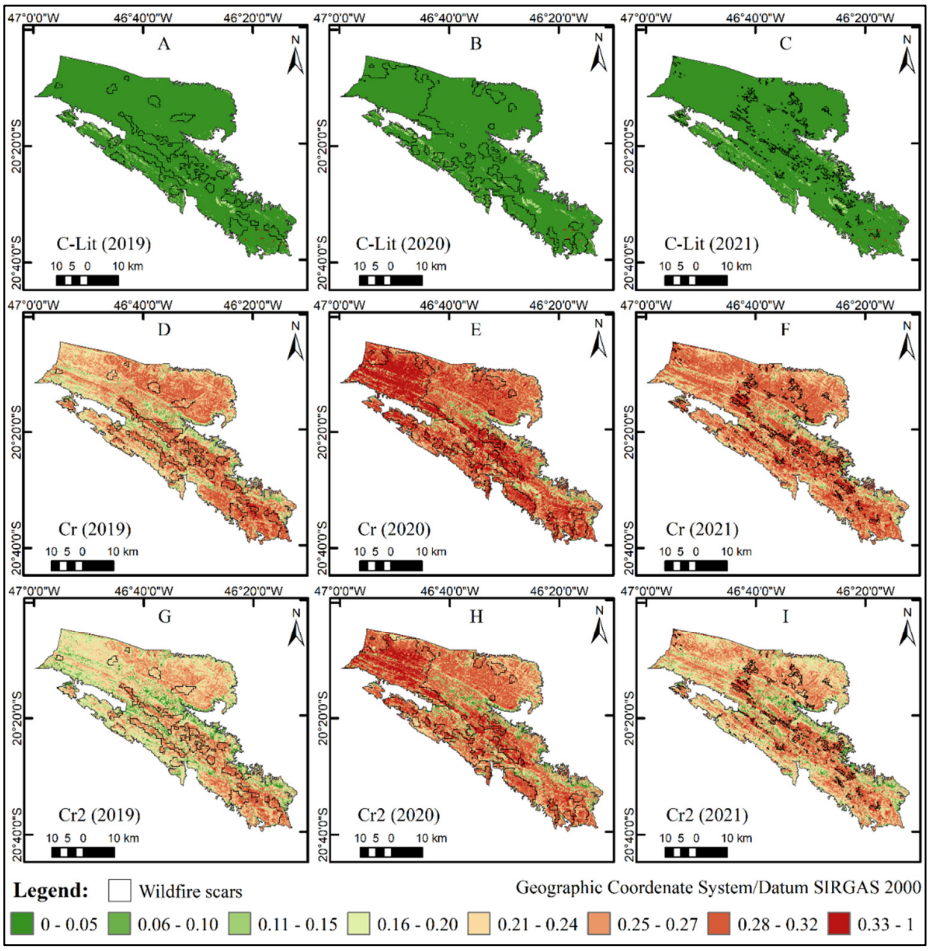

Figure 6. Maps of C factors for Serra da Canastra National Park. (A) C-Lit factor in 2019; (B) C-Lit factor in 2020; (C) C-Lit factor in 2021; (D) Cr factor in 2019; (E) Cr factor in 2020; (F) Cr factor in 2021; (G) Cr2 factor in 2019; (H) Cr2 factor in 2020; (I) Cr2 factor in 2021

Table 5. The soil loss rate in the Serra da Canastra National Park from 2019 to 2021 using different C factors

Use and coverage	2019			2020			2021		
	C-Lit	Cr	Cr2	C-Lit	Cr	Cr2	C-Lit	Cr	Cr2
	Mg ha^{-1} yr^{-1}								
Forest formation	0.11	2.99	2.26	0.12	3.41	3.33	0.11	3.58	3.20
Cerrado formation	0.20	13.63	12.14	0.21	14.67	15.83	0.18	13.73	13.35
Forest plantation	-	-	-	0.98	4.01	3.60	0.49	4.94	4.26
Grassland	1.00	8.81	8.21	1.15	9.39	10.22	0.22	8.91	8.93
Pasture	3.25	13.98	12.80	3.25	14.66	16.08	0.81	13.93	13.80
Sugarcane	3.50	6.59	6.22	3.03	5.96	6.93	3.79	7.46	7.61
Mosaic of uses	9.97	14.87	13.18	9.71	15.70	16.98	9.64	14.74	14.33
Other non-vegetated areas	71.84	26.08	25.36	67.12	24.50	25.51	67.47	23.92	24.79
Soybean	2.56	4.61	4.33	2.50	4.52	4.32	2.49	4.51	4.51
Other temporary crops	3.77	6.26	5.75	4.09	7.31	8.33	3.93	6.95	6.88
Coffee	4.35	8.27	5.02	4.24	5.82	5.96	4.35	5.82	5.38
Citrus	13.25	21.69	19.71	12.98	23.25	24.42	12.84	21.17	20.98
Average Loss	0.75	10.94	9.99	1.00	11.54	12.55	0.88	11.03	10.91

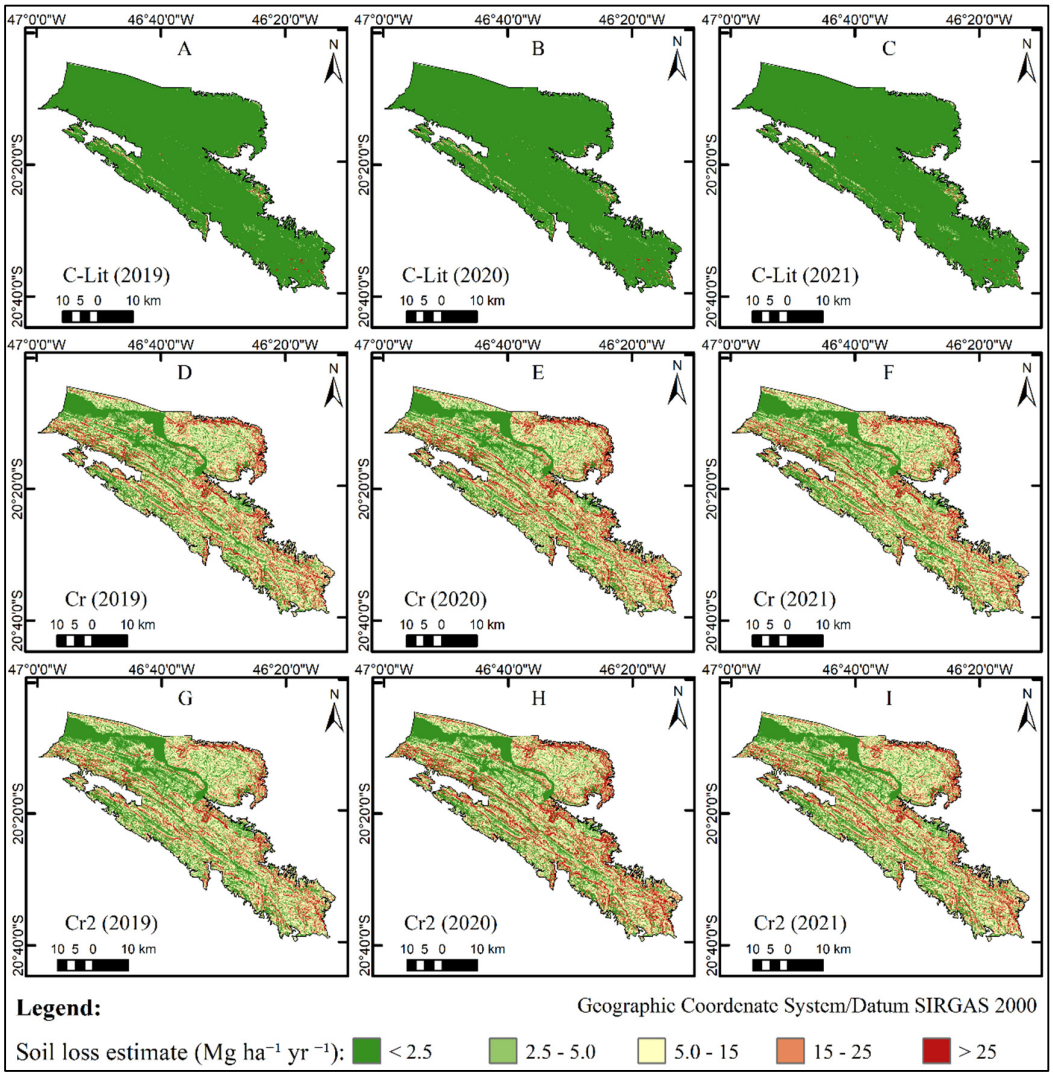

Figure 7. Maps of soil loss estimates from C factors for Serra da Canastra National Park. (A) C-Lit factor in 2019; (B) C-Lit factor in 2020; (C) C-Lit factor in 2021; (D) Cr factor in 2019; (E) Cr factor in 2020; (F) Cr factor in 2021; (G) Cr2 factor in 2019; (H) Cr2 factor in 2020; (I) Cr2 factor in 2021

The spatialization of soil loss rates revealed differences between methodologies for obtaining the C factor. C-Lit showed lower values, leading to greater homogeneity in susceptibility to soil loss (Table 6 and Figures 7A, 7B, 7C). On the other hand, Cr and Cr2 showed higher soil loss rates (Table 6 and Figures 7D, 7E, 7F, 7G, 7H, and 7I). The intervals of soil loss rates (Figure 7) are based on Avanzi *et al.* (2013).

High susceptibilities to water erosion are found in areas that commonly have shallow soils, fertility limitations, and high erodibility (Vasconcelos *et al.*, 2012), such as Cambisols and Neosols. The water infiltration rate in the soil is influenced by the topography, where poorly drained soils are more susceptible to water erosion. Therefore, it is essential to consider soil drainage in the planning of sustainable management practices (Castro and Hernani, 2015).

Vegetative cover plays a fundamental role in soil protection against water erosion, reducing the impact of rainfall, increasing water infiltration rates, and decreasing runoff (Bertoni *et al.*, 2012). Additionally, vegetation contributes to soil stability and improves its structure (Qian *et al.*, 2022; Zhang *et al.*, 2022).

Therefore, the preservation and sustainable management of vegetative cover are essential for the conservation of natural resources, especially soil and water.

The correlation between transported sediments and water flow from 2019 to 2021 is illustrated in Figure 8.

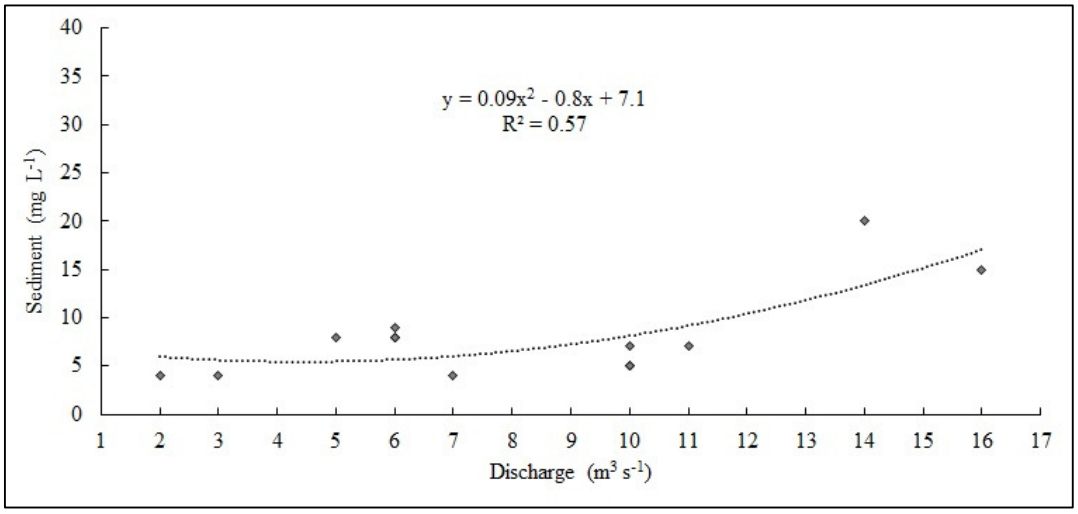

Figure 8. Sediment transport curve × water discharge in the Serra da Canastra National Park, Minas Gerais, Brazil

Despite the limited amount of data available at the hydrosedimentological station, which resulted in a low R^2 adjustment (Figure 8), it was possible to validate soil loss rates based on both observed and estimated sediments by the InVEST model (Table 6).

Table 6. Observed sediment at the hydrosedimentological station, sediment estimated by InVEST, and associated error in the Serra da Canastra National Park

Year	Sediment observed Mg ha^{-1} yr^{-1}	Estimated sediment Mg ha^{-1} yr^{-1}					
		C-Lit	Error %	Cr	Error %	Cr2	Error %
2019	0.021	0.029	38	0.085	300	0.083	295
2020	0.045	0.029	-36	0.086	90	0.088	96
2021	0.015	0.028	93	0.086	470	0.085	467

In Serra da Canastra National Park, sediment generation observed at the hydrosedimentological station ranged from 0.015 to 0.045 Mg ha^{-1} yr^{-1}. Among the methods used to obtain the C factor, C-Lit presented estimated sediment generation values closest to the observed sedimentation rate. NDVI-based C values identify classes most affected by seasonal or wildfire effects with great precision. Thus, lower NDVI values and, consequently, higher C values, result in greater errors in soil loss estimates, as observed in this study (Durigon *et al*., 2014; Macedo *et al*., 2021).

In the park, with the Cr2 factor, there was a slight reduction in soil loss rates compared to those with the Cr factor. However, it is essential to highlight that despite overestimates of soil losses, the Cr and Cr2 factors are effective in identifying areas with greater susceptibility to erosion and, therefore, both methods can be used in conservation planning of the area and in directing practices of mitigation of soil losses. Therefore, the calculation of the C factor from the NDVI is especially important in tropical regions, such as Brazil, where annual climate variation directly conditions the changes in land use and cover, and, in this way, it is possible to identify spatial and temporal variations in the vegetation cover. Furthermore, aiming to minimize errors in soil

loss estimates, new studies on calculating the C factor by remote sensing in Brazilian territory indicate a path of routines that improve the precision of information obtained from satellite images using meteorological data (Almagro *et a*l., 2019; Macedo *et al*., 2021).

In the comparison between sediment measured by the hydrosedimentological station and that estimated by InVEST, it is worth highlighting the effectiveness of the approach, supported by recent studies assessing erosive processes and sediment delivery (Hamel *et al*., 2015; Bouguerra and Jebari, 2017; Matomela *et al*., 2022).

Forest fires and controlled burns are longstanding management practices in the Serra da Canastra National Park, especially during the dry season (Messias and Ferreira, 2019a; 2019b). In the initial years, forest fires may even increase the nutrient content in the soil, which subsequently declines (Agbeshie *et al*., 2022). Over time, soil degradation caused by forest fires intensifies water erosion processes, reduces water infiltration rates, increases soil loss rates, impairs ecosystem services (Depountis *et al*., 2020; Efthimiou *et al.*, 2020; Riquetti *et al*., 2022), and contributes to greenhouse gas emissions (Friedlingstein *et al*., 2015). Therefore, fires and forest fires must be avoided and combated in the area, in addition to the need for correct supervision by the responsible institutions, to prevent fires caused by human action.

Conclusions

The soil loss rates in the park ranged from 0.75 Mg ha^{-1} yr^{-1} to 12.55 Mg ha^{-1} yr^{-1}, according to different methods of obtaining the C factors. The NDVI-derived C factors corresponded to the highest soil loss rates, as they reflect the spectral response of non-homogeneous areas. Forest fires represent abrupt changes in land use and land cover, affecting the spectral response of NDVI and directly increasing the C factor and soil loss rates. The sediment delivery rates calculated by InVEST validated the soil loss rates estimated by RUSLE. The assessment of water erosion in extensive areas, such as the Serra da Canastra National Park, is a necessary tool that contributes to defining the best management techniques for the conservation of natural resources and identifying priority areas for the adoption of degradation mitigation measures.

Authors' Contributions

Conceptualization: GSR, RLM; Data curation: GSR, GHEL; Formal analysis: RLM, JEBA, GSR; Methodology: GSR; Project administration: RLM, GSR; Software: GSR, DBS, GHEL; Supervision: MRL, JEBA, FGR; Validation: GHEL; Visualization: GSR; Writing - original draft: GSR; Writing - review and editing: GSR, DBS, GHEL, FGR, JEBA, RLM. All authors read and approved the final manuscript.

Ethical approval (for researches involving animals or humans)

Not applicable.

Acknowledgements

The authors thank the "Coordenação de Aperfeiçoamento de Pessoal de Nível Superior – Brazil (CAPES) for the scholarship offered to the first author. To the "Fundação de Amparo à Pesquisa do Estado de Minas Gerais - Brazil" (FAPEMIG) for the scholarship offered to the third author. This study was financed in

part by the Coordenação de Aperfeiçoamento de Pessoal de Nível Superior – Brazil (CAPES) – Finance Code 001.

Conflict of Interests

The authors declare that there are no conflicts of interest related to this article.

References

Agbeshie AA, Abugre S, Atta-Darkwa T, Awuah R (2022). A review of the effects of forest fire on soil properties. Journal of Forestry Research 33(5):1419-1441. *https://doi.org/10.1007/s11676-022-01475-4*

Almagro A, Thomé TC, Colman CB, Pereira RB, Marcato Junior J, Rodrigues DBB (2019). Improving cover and management factor (C-factor) estimation using remote sensing approaches for tropical regions. International Soil and Water Conservation Research 7(4):325-334. *https://doi.org/10.1016/j.iswcr.2019.08.005*

Alvares CA, Stape JL, Sentelhas PC, Gonçalves JDM, Sparovek G (2013). Köppen's climate classification map for Brazil. Meteorologische Zeitschrift 22(6):711-728. *https://doi.org/10.1127/0941-2948/2013/0507*

ANA - Agência Nacional de Águas e Saneamento Básico (2023). Retrieved 2023 August 12 from: *https://www.snirh.gov.br/hidroweb/mapa*

Andrade NS, Martins Filho MV, Torres JL, Pereira GT, Marques Júnior J (2011). Impacto técnico e econômico das perdas de solo e nutrientes por erosão no cultivo da cana-de-açúcar [Technical and economic impact of soil and nutrient losses due to erosion in sugarcane cultivation.]. Engenharia Agrícola 31:539-550. *https://doi.org/10.1590/S0100-69162011000300014*

Avanzi JC, Silva, MLN, Curi N, Norton, LD, Beskow S, Martins SG (2013). Spatial distribution of water erosion risk in a watershed with eucalyptus and Atlantic Forest. Ciência e Agrotecnologia 37(5):427-434. *https://doi.org/10.1590/S1413-70542013000500006*

Ayer JEB, Olivetti D, Mincato RL, Silva MLN (2015). Erosão hídrica em Latossolos Vermelhos distróficos. [Water erosion in dystrophic Red Latosols] Pesquisa Agropecuária Tropical 45:180-191. *https://doi.org/10.1590/1983-40632015v4531197*

Barbosa BDS, Ferraz GAS, Gonçalves LM, Marin DB, Maciel DT, Ferraz PFP, Rossi G (2019). RGB vegetation indices applied to grass monitoring: a qualitative analysis. Agronomy Research 17(2):349-357. *https://doi.org/10.15159/ar.19.119*

Batista PVG, Silva MLN, Silva BPC, Curi N, Bueno IT, Acerbi Júnior FW, ... Quinton J (2017). Modelling spatially distributed soil losses and sediment yield in the upper Grande River Basin-Brazil. Catena 157:139-150. *https://doi.org/10.1016/j.catena.2017.05.025*

Bertol I, Cassol EA, Merten GH (2019). Manejo e conservação do solo e da água [Soil and water management and conservation] (1th ed), Viçosa-MG.

Bertol I, Schick J, Batistela O (2001). Razão de perdas de solo e fator C para as culturas de soja e trigo em três sistemas de preparo em um Cambissolo Húmico alumínico [Soil loss ratio and C factor for soybean and wheat crops in three tillage systems in an aluminum humic Cambisol]. Revista Brasileira de Ciência do Solo 25:451-461. *https://doi.org/10.1590/S0100-06832001000200021*

Bertoni J, Lombardi Neto F (2012). Conservação do solo [Soil conservation] (10th ed), Piracicaba-SP.

Beskow S, Mello CR, Norton LD, Curi N, Viola MR, Avanzi JC (2009). Soil erosion prediction in the Grande River Basin, Brazil using distributed modeling. Catena 79(1):49-59. *https://doi.org/10.1016/j.catena.2009.05.010*

Borrelli P, Robinson DA, Panagos P, Lugato E, Yang JE, Alewell C, ... Ballabio, C (2020). Land use and climate change impacts on global soil erosion by water (2015-2070). Proceedings of the National Academy of Sciences 117(36):21994-22001. *https://doi.org/10.1073/pnas.2001403117*

Bouguerra S, Jebari S (2017). Identification and prioritization of sub-watersheds for land and water management using InVEST SDR model: Rmelriver basin, Tunisia. Arabian Journal of Geosciences 10:1-9. *https://doi.org/10.1007/s12517-017-3104-z*

Brasil (1972). Decreto n° 70.355, de 3 de abril de 1972. Cria o Parque Nacional da Serra da Canastra, no Estado de Minas Gerais, com os limites que especifica, e dá outras providências [Creation of the Serra da Canastra National Park, in the State of Minas Gerais, with the limits it specifies, and provides other measures]. Retrieved 2023 March 11 from: *https://www.planalto.gov.br/ccivil_03/decreto/1970-1979/D70355.htm*

Brasil (2000). Sistema Nacional de Unidades de Conservação da Natureza: Lei n.º 9.985, de 18 de julho de 2000 [National System of Nature Conservation Units: Law No. 9,985, of July 18, 2000]. Retrieved 2023 March 11 from: *https://www.planalto.gov.br/ccivil_03/leis/l9985.htm*

Brasil (2005). Ministério do Meio Ambiente. Instituto Brasileiro Meio Ambiente e Recursos Naturais Renováveis. Plano de manejo do Parque Nacional da Serra da Canastra [Brazilian Institute for the Environment and Renewable Natural Resources. Serra da Canastra National Park management plan] Retrieved 2023 March 11 from: *http://www.icmbio.gov.br/portal/images/stories/imgs-unidades-coservacao/pm_parna_serra_canastra_1.pdf*

Cabral JBP, Becegato VA, Scopel I, Lopes RM (2005). Uso de técnicas de geoprocessamento para mapear o potencial natural de erosão da chuva na bacia hidrográfica do reservatório de Cachoeira Dourada GO/MG [Use of geoprocessing techniques to map the natural potential for rain erosion in the watershed of the Cachoeira Dourada GO/MG]. Raega-O Espaço Geográfico em Análise 10:107-116. *http://dx.doi.org/10.5380/raega.v10i0.4982*

Cardoso P H, Menini Neto L, Salimena FRG (2019). Stachytarpheta grandiflora, a new species of Verbenaceae from the Parque Nacional da Serra da Canastra, Minas Gerais, Brazil. Phytotaxa 413(1):61-66. *https://doi.org/10.11646/phytotaxa.413.1.7*

Castro RM, Alves WS, Oliveira Marcionilio SML, Moura DMB, Oliveira, DMS (2022). Soil losses related to land use and rainfall seasonality in a watershed in the Brazilian Cerrado. Journal of South American Earth Sciences 119:104020. *https://doi.org/10.1016/j.jsames.2022.104020*

Castro SS, Hernani LC (2015). Solos frágeis: caracterização, manejo e sustentabilidade. Embrapa Solos-Livro técnico (INFOTECA-E) [Fragile soils: characterization, management and sustainability. Embrapa Soils-Technical book (INFOTECA-E)]. Retrieved 2023 March 17 from: *https://www.infoteca.cnptia.embrapa.br/handle/doc/1039217*

Costa L, Nunes L, Ampatzidis Y (2020). A new visible band index (vNDVI) for estimating NDVI values on RGB images utilizing genetic algorithms. Computers and Electronics in Agriculture 172:105334. *https://doi.org/10.1016/j.compag.2020.105334*

Coutinho LM (2006). The biome concept. Acta Botanica Brasilica 20:13-23. *https://doi.org/10.1590/S0102-33062006000100002*

Cunha ER, Bacani VM,Panachuki E (2017). Modeling soil erosion using RUSLE and GIS in a watershed occupied by rural settlement in the Brazilian Cerrado. Natural Hazards 85(2):851-868. *https://doi.org/10.1007/s11069-016-2607-3*

Dechen SCF, Telles TS, Guimarães MDF, Maria ICD (2015). Perdas e custos associados à erosão hídrica em função de taxas de cobertura do solo [Losses and costs associated with water erosion depending on soil cover rates]. Bragantia 74:224-233. *https://doi.org/10.1590/1678-4499.0363*

Depountis N, Michalopoulou M, Kavoura K, Nikolakopoulos K, Sabatakakis N (2020). Estimate changes in soil erosion rate in areas affected by wildfires. ISPRS International Journal of Geo-Information 9(10):562-580. *https://doi.org/10.3390/ijgi9100562*

Durigan G, Ratter JA (2016). The need for a consistent fire policy for Cerrado conservation. Journal of Applied Ecology 53(1):11-15. *https://doi.org/10.1111/1365-2664.12559*

Durigon VL, Carvalho DF, Antunes MAH, Oliveira PTS, Fernandes MM (2014). NDVI time series for monitoring RUSLE cover management factor in a tropical watershed. International Journal of Remote Sensing 35(2):441-453. *https://doi.org/10.1080/01431161.2013.871081*

Efthimiou N, Psomiadis E, Panagos P (2020). Fire severity and soil erosion susceptibility mapping using multi-temporal Earth Observation data: The case of Mati fatal wildfire in Eastern Attica, Greece. Catena 187:104320. *https://doi.org/10.1016/j.catena.2019.104320*

Esri (2021). ArcGIS Desktop: Release 10.8.2 [Software].

Farinasso M, Carvalho Júnior OA, Guimarães RF, Gomes RAT, Ramos VM (2006). Avaliação Qualitativa do Potencial de Erosão Laminar em Grandes Áreas por Meio da EUPS Equação Universal de Perdas de Solos Utilizando Novas Metodologias em SIG para os Cálculos dos seus Fatores na Região do Alto Parnaíba PI-MA [Qualitative Assessment of Laminar Erosion Potential in Large Areas Using EUPS Universal Soil Loss Equation Using New GIS Methodologies to Calculate Factors in the Alto Parnaíba PI-MA Region]. Revista Brasileira De Geomorfologia 7(2):75-85. *https://doi.org/10.20502/rbg.v7i2.80*

Farr TG, Rosen PA, Caro E, Crippen R, Duren R, Hensley S, Alsdorf D (2007). The shuttle radar topography mission. Reviews of Geophysics 45(2):1-33. *https://doi.org/10.1029/2005RG000183*

Félix FC, Cândido BM, Moraes JFL (2023). How suitable are vegetation indices for estimating the (R) USLE C-factor for croplands? A case study from Southeast Brazil. ISPRS Open Journal of Photogrammetry and Remote Sensing 10:100050. *https://doi.org/10.1016/j.ophoto.2023.100050*

Friedlingstein P (2015). Carbon cycle feedbacks and future climate change. Philosophical Transactions of the Royal Society A: Mathematical, Physical and Engineering Sciences 373(2054):20140421. *https://doi.org/10.1098/rsta.2014.0421*

Funk C, Peterson P, Landsfeld M, Pedreros D, Verdin J, Shukla S, Michaelsen J (2015). The climate hazards infrared precipitation with stations – a new environmental record for monitoring extremes. Scientific Data 2(1):1-21. *https://doi.org/10.1038/sdata.2015.66*

Gil HAP, Pacheco AJM (2020). RGB Spectral indices for the analysis of soil protection by vegetation cover against erosive processes. In: Soil Erosion-Current Challenges and Future Perspectives in a Changing World. IntechOpen. London pp 3-14.

Gorelick N, Hancher M, Dixon M, Ilyushchenko S, Thau D, Moore, R. (2017). Google Earth Engine: Planetary-scale geospatial analysis for everyone. Remote Sensing of Environment 202:18-27. *https://doi.org/10.1016/j.rse.2017.06.031*

Gwapedza D, Hughes DA, Slaughter AR Mantel SK (2021). Temporal Influences of Vegetation Cover (C) Dynamism on MUSLE Sediment Yield Estimates: NDVI Evaluation. Water 13(19):2707. *https://doi.org/10.3390/w13192707*

Hamel P, Chaplin-Kramer R, Sim S Mueller C (2015). A new approach to modeling the sediment retention service (InVEST 3.0): Case study of the Cape Fear catchment, North Carolina, USA. Science of the Total Environment 524:166-177. *https://doi.org/10.1016/j.scitotenv.2015.04.027*

Hasui Y (2010). A grande colisão pré-cambriana do sudeste brasileiro e a estruturação regional [The great Precambrian collision in southeastern Brazil and regional structuring]. Geociências 29(2):141-169.

Hysa A, Spalevic V, Dudic B, Roșca S, Kuriqi A, Bilașco Ș, Sestras P (2021). Utilizing the available open-source remotely sensed data in assessing the wildfire ignition and spread capacities of vegetated surfaces in Romania. Remote Sensing 13(14):2737. *https://doi.org/10.3390/rs13142737*

IBGE - Instituto Brasileiro de Geografia e Estatística (2022). Coordenação de Estruturas Territoriais. Malha municipal digital e áreas territoriais [Coordination of Territorial Structures. Digital municipal network and territorial areas]. Retrieved 2023 August 16 from: *https://www.ibge.gov.br/geociencias/organizacao-do-territorio/malhas-territoriais/15774-malhas.html*

IUSS - International Union of Soil Sciences (2014). World reference base for soil resources 2014. In: Schad P, van Huyssteen C, Micheli E (Eds). World Soil Resources Reports. No. 106. Food and Agriculture Organization of the United Nations FAO, Rome 106:1-203 Retrieved 2023 August 16 from: *https://www.fao.org/3/i3794en/I3794en.pdf*

Klink CA, Machado RB (2005). A conservação do Cerrado brasileiro [The conservation of the Brazilian Cerrado]. Megadiversidade 1(1):147-155.

Lal R (2020). Soil erosion and gaseous emissions. Applied Sciences 10(8):2784. *https://doi.org/10.3390/app10082784*

Lanorte A, Cillis G, Calamita G, Nolè G, Pilogallo A, Tucci B, De Santis F (2019). Integrated approach of RUSLE, GIS and ESA Sentinel-2 satellite data for post-fire soil erosion assessment in Basilicata region (Southern Italy). Geomatics, Natural Hazards and Risk 10(1):1563-1595. *https://doi.org/10.1080/19475705.2019.1578271*

Lense GHE, Parreiras TC, Spalevic V, Avanz, JC, Mincato RL (2021). Soil losses in the State of Rondônia, Brazil. Ciência Rural 51(5):6. *https://doi.org/10.1590/0103-8478cr20200460*

Liu B, Xie Y, Li Z, Liang Y, Zhang W, Fu S, Guo Q (2020). The assessment of soil loss by water erosion in China. International Soil and Water Conservation Research 8(4):430-439. *https://doi.org/10.1016/j.iswcr.2020.07.002*

Macedo PMS, Oliveira PTS, Antunes MAH, Durigon VL, Fidalgo ECC, Carvalho DF (2021). New approach for obtaining the C-factor of RUSLE considering the seasonal effect of rainfalls on vegetation cover. International Soil and Water Conservation Research 9(2):207-216. *https://doi.org/10.1016/j.iswcr.2020.12.001*

Macêdo RJA, Santos JC, Surya L (2021). Modelagem da erosão hídrica potencial no Parque Nacional Serra da Capivara, Nordeste do Brasil [Modeling potential water erosion in Serra da Capivara National Park, Northeast Brazil]. Revista Brasileira de Geomorfologia 22(4):793-808. *https://doi.org/10.20502/rbg.v22i4.1942*

Mannigel AR, Passos M, Moreti D, Medeiros LR (2002). Fator erodibilidade e tolerância de perda dos solos do Estado de São Paulo [Erodibility factor and loss tolerance of soils in the State of São Paulo]. Acta Scientiarum Agronomy 24:1335-1340. *https://doi.org/10.4025/actasciagron.v24i0.2374*

Mapbiomas (2022). Projeto Mapbiomas. Mapeamento das áreas queimadas no Brasil (Coleção 1) [Mapping of burned areas in Brazil (Collection 1)]. Retrieved 2023 July 11 from: *https://plataforma.mapbiomas.org*

Mapbiomas (2023). Projeto Mapbiomas. Coleção [7] da Série Anual de Mapas de Uso e Cobertura da Terra do Brasil [Collection [7] of the Annual Series of Land Use and Cover Maps of Brazil]. Retrieved 2023 July 11 from: *https://plataforma.mapbiomas.org*

Martins SG, Silva MLN, Avanzi JC, Curi N, Fonseca S (2010). Fator cobertura e manejo do solo e perdas de solo e água em cultivo de eucalipto e em Mata Atlântica nos Tabuleiros Costeiros do Estado do Espírito Santo [Soil coverage and management factor and soil and water losses in eucalyptus cultivation and in the Atlantic Forest in the Coastal Tablelands of the state of Espírito Santo]. Scientia Forestalis 38(87):517-526.

Matomela N, Li T, Ikhumhen HO, Lopes RND, Meng L (2022). Soil erosion spatio-temporal exploration and Geodetection of driving factors using InVEST-sediment delivery ratio and Geodetector models in Dongsheng, China. Geocarto International 37(26):13039-13056. *https://doi.org/10.1080/10106049.2022.2076912*

Mello CD, Viola MR, Beskow S, Norton LD (2013). Multivariate models for annual rainfall erosivity in Brazil. Geoderma 202:88-102. *https://doi.org/10.1016/j.geoderma.2013.03.009*

Messias CG, Ferreira MC (2017). Aplicação do método de classificação contínua fuzzy para o mapeamento da fragilidade do terreno em relação à ocorrência de ravinas no Parque Nacional da Serra da Canastra [Application of continuous fuzzy classification method for mapping terrain fragility regarding the occurrence of gullies in the Serra da Canastra National Park]. RAEGA-O Espaço Geográfico em Análise, 39:111-127. *https://doi.org/10.5380/raega.v39i0.42914*

Messias CG, Ferreira MC (2019a). Análise da distribuição espacial das queimadas no Parque Nacional da Serra da Canastra (MG), entre 1984 e 2017 [Analysis of the spatial distribution of fires in the Serra da Canastra National Park (MG), between 1984 and 2017]. Uberlândia-MG: Caminhos de Geografia 2071:52-71. *https://doi.org/10.14393/RCG207144609*

Messias CG, Ferreira MC (2019b). Modelo Geoespacial para a Identificação de Áreas com Perigo de Propagação de Queimadas no Parque Nacional da Serra da Canastra [Geospatial Model for Identification of Areas with Danger of Spread of Fires in the Serra da Canastra National Park]. Revista do Departamento De Geografia 38:154-168. *https://doi.org/10.11606/rdg.v38i1.153493*

Moore ID, Burch GJ (1986). Physical basis of the length-slope factor in the universal soil loss equation. Soil Science Society of America Journal 50(5):1294-1298. *https://doi.org/10.2136/sssaj1986.03615995005000050042x*

Morais RCS, Sales MCL (2017). Estimativa do potencial natural de erosão dos solos da bacia hidrográfica do Alto Gurguéia, Piauí-Brasil, com uso de Sistema de Informação Geográfica [Estimation of the natural potential for soil erosion in the Alto Gurguéia river basin, Piauí-Brazil, using a Geographic Information System]. Caderno de Geografia 27(1):84-105. *https://doi.org/10.5752/p.2318-2962.2017v27nesp1p84*

Nachtigall SD, Nunes MCM, Moura-Bueno JM, Lima CLRD, Miguel P, Beskow S, Silva TP (2020). Spatial modeling of soil water erosion associated with agroclimatic seasonality in the southern region of Rio Grande do Sul, Brazil. Engenharia Sanitaria e Ambiental 25:933-946. *https://doi.org/10.1590/S1413-41522020201901 36*

Nanzad L, Zhang J, Tuvdendorj B, Nabil M, Zhang S, Bai Y (2019). NDVI anomaly for drought monitoring and its correlation with climate factors over Mongolia from 2000 to 2016. Journal of Arid Environments 164:69-77. *https://doi.org/10.1016/j.jaridenv.2019.01.019*

Novaes GT, Brito JLS, Fábio OS (2018). Unidades climáticas do Triângulo Mineiro/Alto Paranaíba. Revista Brasileira de Climatologia [Climatic units of the Triângulo Mineiro/Alto Paranaíba. Brazilian Journal of Climatology] 23:223-243. *https://doi.org/10.5380/abclima.v23i0.58520*

Panagos P, Borrelli P, Meusburger K, Alewell C, Lugato E, Montanarella L (2015). Estimating the soil erosion covermanagement factor at the European scale. Land Use Policy 48:38-50. *https://10.1016/j.landusepol.2015.05.021*

Pettorelli N, Vik JO, Mysterud A, Gaillard JM, Tucker CJ, Stenseth NC (2005). Using the satellite-derived NDVI to assess ecological responses to environmental change. Trends in Ecology & Evolution 20(9):503-510. *https://doi.org/10.1016/j.tree.2005.05.011*

Polidoro JC, Freitas PL, Hernani LC, Anjos LHCD, Rodrigues RDAR, Cesário FV, Ribeiro JL (2021). Potential impact of plans and policies based on the principles of conservation agriculture on the control of soil erosion in Brazil. Land Degradation & Development 32(12):3457-3468. *https://doi.org/10.1002/ldr.3876*

Qian K, Ma X, Wang Y, Yuan X, Yan W, Liu Y, Yang X, ... Li J (2022). Effects of vegetation change on soil erosion by water in major basins, Central Asia. Remote Sensing 14(21):5507. *https://doi.org/10.3390/rs14215507*

Renard KG, Foster GR, Weesier GA, Mccool DK, Yoder DC (1997). Predicting soil erosion by water: a guide to conservation planning with the Revised Universal Soil Loss Equation (RUSLE). US Department of Agriculture, Agricultural Research Service.

Riquetti NB, Mello CR, Leandro D, Guzman JA, Beskow S (2022). Assessment of the soil-erosion-sediment for sustainable development of South America. Journal of Environmental Management 321:1-15. *https://doi.org/10.1016/j.jenvman.2022.115933*

Rodrigues WF, Costa IG (2021). Danos ambientais provocados por incêndios no Cerrado: uma análise entre os anos de 2004 e 2019 no Parque Nacional da Serra da Canastra-MG [Environmental damage caused by fires in the Cerrado: an analysis between 2004 and 2019 in the Serra da Canastra National Park-MG]. Ensaios de Geografia 7(14):163-188. *https://doi.org/10.22409/eg.v7i14.48500*

Roose EJ (1977). Application of the Universal Soil Loss Equation of Wischmeier and Smith in West Africa. In: Greenland DJ, Lal R (Eds). Soil conservation and management in the humid tropics Chichester: John Wiley & Sons pp 177-187.

Rouse JW, Haas RH, Schell JA, Deering DW (1974). Monitoring vegetation systems in the Great Plains with ERTS. NASA Spec. Publ 351(1):309-329.

Salgado AAR, Santos LJC, Paisani JC (2019). The physical geography of Brazil: Environment, vegetation and landscape. Springer Nature Switzerland: Springer Publisher 1:93-117 *https://doi.org/10.1007/978-3-030-04333-9*

Sano EE, Bettiol GM, Martins EDS, Couto Júnior AF, Vasconcelos V, Bolfe EL, Victoria DDC (2020). Características gerais da paisagem do Cerrado. In: Dinâmica agrícola no cerrado: análises e projeções [General characteristics of the Cerrado landscape. In: Agricultural dynamics in the cerrado: analyzes and projections]. Embrapa Cerrados, Brasília pp 21-37.

Santana DB, Bolleli TM, Lense GHE, Silva LFPM, Sestras P, Spalevic V, Mincato RL (2021). Estimate of water erosion in coffee growing areas in Serra da Mantiqueira, Minas Gerais State, Brazil. Agriculture and Forestry 67(2):75-88. *https://10.17707/AgricultForest.67.2.06*

Senanayake S, Pradhan B, Alamri A, Park HJ (2022). A new application of deep neural network (LSTM) and RUSLE models in soil erosion prediction. Science of the Total Environment 845:157220. *https://doi.org/10.1016/j.scitotenv.2022.157220*

Sestras P, Mircea S, Cîmpeanu SM, Teodorescu R, Roșca S, Bilașco Ș, ... Spalevic V (2023). Soil erosion assessment using the intensity of erosion and outflow model by estimating sediment yield: Case Study in river basins with different characteristics from Cluj County, Romania. Applied Sciences 13(16):9481. *https://doi.org/10.3390/app13169481*

Seutloali KE, Beckedahl HR (2015). A review of road-related soil erosion: an assessment of causes, evaluation techniques and available control measures. Earth Sciences Research Journal 19(1):73-80. *https://10.15446/esrj.v19n1.43841*

Shakesby RA (2011). Post-wildfire soil erosion in the Mediterranean: Review and future research directions. Earth-Science Reviews 105(3/4)71-100. *https://doi.org/10.1016/j.earscirev.2011.01.001*

Sharp R, Chaplin-Kramer R, Wood S, Guerry A, Tallis H, Ricketts T, ... Douglass J (2018). InVEST 3.5.0 User's Guide. California: The Natural Capital Project. Stanford University, University of Minnesota, The Nature Conservancy, and World Wildlife Fund. *https://doi.org/10.13140/RG.2.2.32693.78567*

Silva AL, Souza C, E'loy L, Passos CJS (2019). Selective environmental policies and expansion of the agricultural frontier in the Cerrado: impacts on local communities in a Conservation Unit in western Bahia. Revista Nera (47):321–347. *https://doi.org/10.47946/rnera.v0i47.6274*

Silva AMD, Silva MLN, Curi N, Avanzi JC, Ferreira MM (2009). Erosividade da chuva e erodibilidade de Cambissolo e Latossolo na região de Lavras, sul de Minas Gerais [Rain erosivity and erodibility of Cambisol and Oxisol in the Lavras region, south of Minas Gerais]. Revista Brasileira de Ciência do Solo 33(6):1811-1820. *https://doi.org/10.1590/S0100-06832009000600029*

Silva FGB, Minotti RT, Lombardi Neto F, Primavesi, O, Crestana S. (2010). Previsão da perda de solo na Fazenda Canchim-SP (EMBRAPA) utilizando geoprocessamento e o USLE 2D [Prediction of soil loss at Fazenda Canchim-SP (EMBRAPA) using geoprocessing and USLE 2D]. Engenharia Sanitária e Ambiental 15:141-148. *https://doi.org/10.1590/S1413-41 52201000020000*

Silva MA, Pinto CP, Pinheiro MAP, Marinho MS, Lombello JC, Pinho JMMP, Goulart LEA, Magalhães JR (2020). Mapa geológico do estado de Minas Gerais. Belo Horizonte: Companhia de Pesquisa de Recursos Minerais CPRM. 1 mapa, color. Escala 1:1.000.000 [Geological map of the state of Minas Gerais. Belo Horizonte: Mineral Resources Research Company CPRM. 1 map, color. Scale 1:1,000,000.] Retrieved 2023 August 14 from: *https://rigeo.sgb.gov.br/handle/doc/21828*

Souza CMP, Veloso GV, Mello CRD, Ribeiro RP, Silva LAP, Leite ME, Fernandes Filho EI (2022). Spatiotemporal prediction of rainfall erosivity by machine learning in southeastern Brazil. Geocarto International 37(26):11652-11670. *https://doi.org/10.1080/10106049.2022.2060318*

UFV Universidade Federal de Viçosa, Fundação Centro Tecnológico de Minas Gerais CETEC, Universidade Federal de Lavras UFLA, Fundação Estadual do Meio Ambiente FEAM (2010). Mapa de solos do Estado de Minas Gerais Escala 1:650.000 [Soil map of the State of Minas Gerais Scale 1:650,000]. Retrieved 2023 August 14 from: *http://www.feam.br/noticias/1/949-mapas-de-solo-do-estado-de-minas-gerais*

USGS United States Geological Survey (2019). Landsat 8 Surface Reflectance 30 meter (Version 1.5.0). USGS Earth Resources Observation and Science (EROS) Center. Retrieved 2023 February 16 from: *https://earthexplorer.usgs.gov*

Valkanou K, Karymbalis E, Bathrellos G, Skilodimou H, Tsanakas K, Papanastassiou D, Gaki-Papanastassiou K (2022). Soil loss potential assessment for natural and post-fire conditions in Evia Island, Greece. Geosciences 12(10):367. *https://doi.org/10.3390/geosciences12100367*

Vasconcelos V, Carvalho Junior OA, Martins ES, Couto Junior AF, Guimarães RF, Gomes RAT (2012). Sistema de classificação geomorfométrica baseado em uma arquitetura sequencial em duas etapas: árvore de decisão e classificador espectral, no Parque Nacional da Serra da Canastra [Geomorphometric classification system based on a two-step sequential architecture: decision tree and spectral classifier, in the Serra da Canastra National Park]. Revista Brasileira De Geomorfologia 13(2):171-186 *https://doi.org/10.20502/rbg.v13i2.248*

Vigiak O, Borselli L, Newham L, McInnes J, Roberts A (2012). Comparison of conceptual landscape metrics to define hillslope-scale sediment delivery ratio. Geomorphology 138(1):74-88. *https://doi.org/10.1016/j.geomorph.2011.08.026*

Wischmeier WH, Smith DD (1978). Predicting rainfall erosion losses: a guide to conservation planning. The USDA Agricultural Handbook (537th ed), Maryland.

Zanter K (2019). Landsat 8-9, Collection 2 (C2), Level 2 Science Product (L2SP) Guide. Surface Reflectance Code (LASRC - Version 5.0) Product Guide. USGS: Sioux Falls, SD, USA. Retrieved 2023 February 16 from: *https://www.usgs.gov/media/files/landsat-8-9-collection-2-level-2-science-product-guide*

Zhang X, Friedl MA, Schaaf CB, Strahler AH, Hodges JCF, Gao F, Reed BC (2016). Monitoring vegetation phenology using MODIS. Remote Sensing of Environment 84(3):471-475. *https://doi.org/10.1016/S0034-4257(02)00135-9*

Zhang X, Song J, Wang Y, Sun H, Li Q (2022). Threshold effects of vegetation coverage on runoff and soil loss in the Loess Plateau of China: A meta-analysis. Geoderma 412:115720. *https://doi.org/10.1016/j.geoderma.2022.115720*

Zhu, Z, Woodcock CE (2014). Automated cloud, cloud shadow, and snow detection in multitemporal Landsat data: An algorithm designed specifically for monitoring land cover change. Remote Sensing of Environment 152:217-234. *https://doi.org/10.1016/j.rse.2014.06.012*

Notes:

- Material disclaimer: The authors are fully responsible for their work and they hold sole responsibility for the articles published in the journal.
- Maps and affiliations: The publisher stay neutral with regard to jurisdictional claims in published maps and institutional affiliations.
- Responsibilities: The editors, editorial board and publisher do not assume any responsibility for the article's contents and for the authors' views expressed in their contributions. The statements and opinions published represent the views of the authors or persons to whom they are credited. Publication of research information does not constitute a recommendation or endorsement of products involved.